ELSEVIER

Journal of Hazardous Materials 44 (1995) 127–139

JOURNAL OF HAZARDOUS MATERIALS

Drift-flux correlation disengagement models: Part II – Shape-based correlations for disengagement prediction via churn-turbulent drift-flux correlation

C.M. Sheppard

Chemical Engineering Department; Louisiana Tech University, P.O. Box 10348 TS, Ruston, LA 71272, USA

Received 21 September 1994; accepted 7 April 1995

Abstract

In Part I of this work the theoretical foundation was laid for predicting disengagement via volumetric gas production and an axial void fraction profile. Earlier work indicated for non-foaming systems one of the two drift-flux correlations can be chosen on the basis of viscosity. Herein, for the churn-turbulent drift-flux correlation (low-viscosity system), the dependence average void fraction and dimensionless superficial vapor velocity [1] on vessel shape (e.g., vertical cylinder, horizontal cylinder, or sphere) is explored. There is very little shape dependence and it is quantified below. A simple two-constant correlation is suggested, which satisfies the conditions at low and high dimensionless superficial vapor velocity conditions. Constants are given for vertical cylinders, horizontal cylinders, and spheres for the churn-turbulent drift-flux correlation.

The disengagement model is based on a constant energy generation per unit mass of liquid. Thus, the application to runaway reaction with vaporization is straightforward. The application of the correlation to reactive systems producing gas (i.e., gassy systems) and to those both producing gas and involving vaporization (i.e., hybrid systems) in non-constant cross-sectional area vessels is clarified here. Rating calculation equations are developed, and the calculations are illustrated. For a rating calculation, the maximum gas rate (based on vent capacity) is known. The calculation of maximum average void fraction (i.e., 1-fill ratio) and gas generation per unit of liquid is straightforward. Thus, the rate of reaction (i.e., gas generation) must be found to assure that the vent capacity is sufficient

Keywords: Pressure relief design; Disengagement; Churn-turbulent drift-flux correlation; Void fraction; DIERS; Venting; Two-phase flow

1. Introduction

As discussed in Part I [2], the phase of the vent flow is important for emergency pressure relief system design. If bubbles form and the vessel contents swell to the top, two-phase vent flow will occur. The sonic velocity two-phase flow is a function of void

SSDI 0304-3894(95)00052-6

fraction, and typically it is over an order of magnitude lower than either the liquid or the vapor sonic velocity. Thus, a larger vent is required. Therefore, predicting the void fraction of the two-phase flow and the point of onset and of disengagement (i.e., cessation) is crucial for proper pressure relief device design.

Pseudo-steady state is assumed to predict disengagement, and an appropriate drift-flux correlation is selected. According to Fisher [3], the churn-turbulent drift-flux correlation is appropriate for a system with a viscosity *less* than 100 cP and no tendency to foam. The bubbly drift-flux correlation is appropriate for a system with a viscosity *greater* than 100 cP and no tendency to foam [3]. This article is devoted to using the churn-turbulent drift-flux correlation to predict disengagement. The results discussed here are applicable to both methods of calculating bubble rise velocity.

A vapor material balance can be formulated with the pseudo-steady-state assumption. This balance can be integrated to find the initial void fraction such that the contents swell up to the top of the vessel. In this article, a correlation equation for the numeric integration results is proposed. This two-constant correlation exactly satisfies the conditions at extremes (i.e., low and high dimensionless superficial vapor velocities). The correlation is fit using numeric integration data for each shape (i.e., vertical cylinders, horizontal cylinders, and spheres). These correlations agree with the average void fractions in regions of interest (i.e., intermediate dimensionless superficial vapor velocities) within a few percentage points.

2. Discussion

2.1. Shape-based correlations

An explicit analytical solution exists for the constant cross-sectional area cases, and numeric integration results exist for the horizontal cylinders and spheres. However, explicit correlations would be more convenient. Therefore, the correlation equation was fit for the vertical cylinder data (i.e., constant cross-sectional area), and for horizontal cylinder and sphere data (i.e., non-constant cross-sectional area). The correlation equation selected was as follows:

$$\bar{\alpha} = \frac{\psi^n}{K + Co\psi^n} = [K\psi^{-n} + Co]^{-1}. \tag{1}$$

This equation is after the form suggested by Fauske et al. [4], which for the churn-turbulent drift-flux correlation with a distribution parameter of unity and an exponent of unity is exactly

$$\bar{\alpha} = \frac{\psi}{2 + \psi}. \tag{2}$$

For a non-unity distribution parameter, the relationship was suggested to be approximately

$$\bar{\alpha} \approx \frac{\psi}{2 + Co\psi}. \tag{3}$$

Other forms were investigated, including the one based on the average void fraction for the constant cross-sectional area case. It had the following form [5]:

$$\overline{\alpha}_{\substack{\text{horizontal}\\\text{cylinder}}} = [1 + K\psi^{-n}]\,\bar{\alpha}_{\substack{\text{vertical}\\\text{cylinder}}}. \tag{4}$$

However, for the churn-turbulent drift-flux correlation, the simple two-constant equation was superior.

2.1.1. *Churn-turbulent shape-based correlations for Co values of 1–1.5*

Fig. 1 shows the numerical integration disengagement model results using the churn-turbulent drift-flux correlation for vertical cylinders, horizontal cylinders, and spheres for *Co* values of 1.0. The correlation equation was used to fit the data. The correlation constants, sum of squares' error, and maximum absolute error are given in Table 1 for the vertical cylinder, horizontal cylinder, and sphere correlations. Similarly, for a *Co* value of 1.5, Fig. 2 shows the model results, and Table 2 shows the correlation constants and error. For a vertical cylinder with a *Co* of unity, the original DIERS correlation is the analytic integration solution. The non-cross-sectional area vessels have constant values greater than 2 and exponent values less than unity. Figs. 3, 4, and 5 show the model results and correlation for each shape, respectively, for a *Co* of 1.5. Fig. 5 also contains the original DIERS approximation, the new correlation, and the data. At high dimensionless superficial vapor velocity values, the DIERS

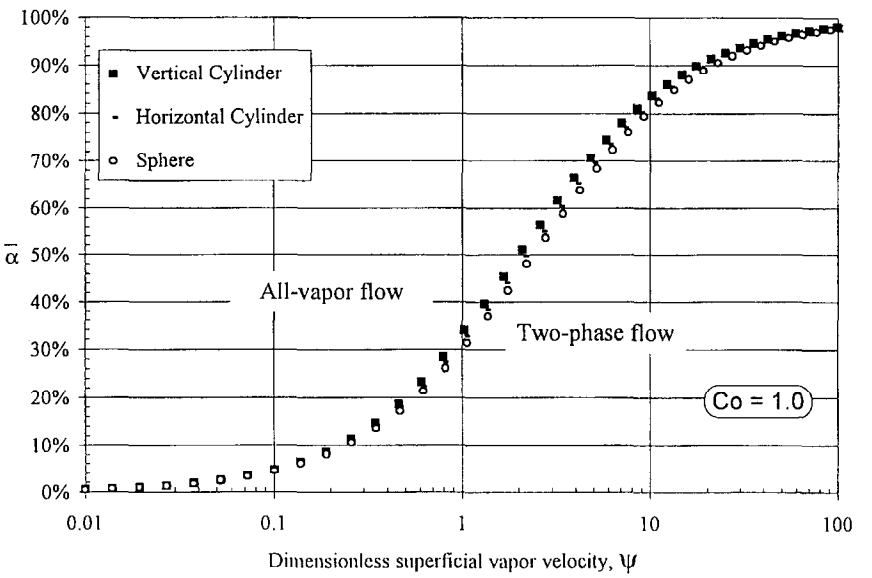

Fig. 1. Churn-turbulent numerical integration disengagement model results for vertical cylinder, horizontal cylinder, and sphere with $Co = 1.0$.

Table 1
Churn-turbulent correlation parameters for $Co = 1.0$ and the correlation equation $\bar{\alpha} = \psi^n/(K + Co\psi^n)$

Shape	Vertical cylinder DIERS approximation	Vertical cylinder	Horizontal cylinder	Sphere
Constant K	2.00	2.20	2.146	2.337
Exponent n	1.00	0.91	0.991	0.982
Sum of squares error	1.10%	0.03%	0.01%	0.01%
Maximum absolute error	0.00%	0.00%	0.19%	0.32%
Number of points	47	47	47	47

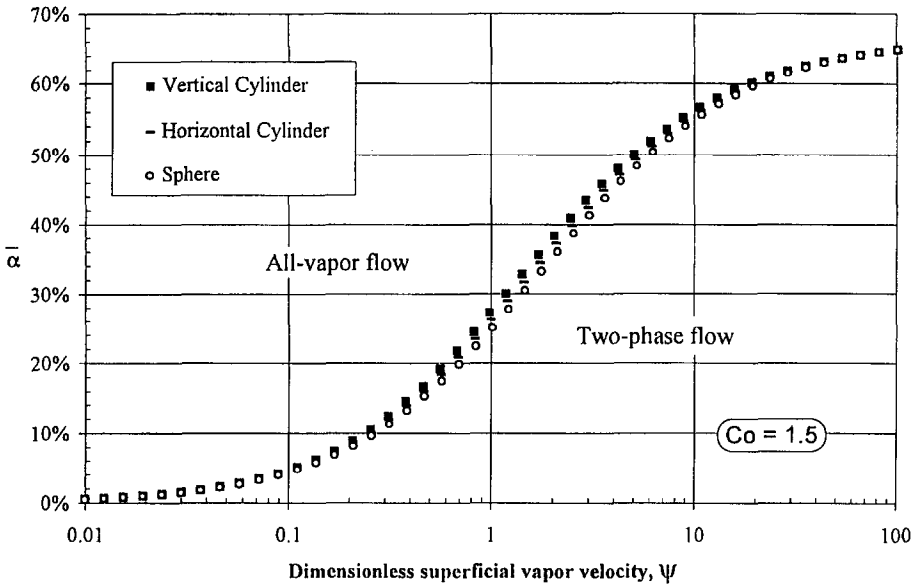

Fig. 2. Churn-turbulent numerical integration disengagement model results for vertical cylinder, horizontal cylinder, and sphere with $Co = 1.5$.

Table 2
Churn-turbulent correlation parameters for $Co = 1.5$ and the correlation equation $\bar{\alpha} = \psi^n/(K + Co\psi^n)$

Shape	Vertical cylinder DIERS approximation	Vertical cylinder	Horizontal cylinder	Sphere
Constant K	2.00	2.20	2.36	2.56
Exponent n	1.00	0.91	0.91	0.91
Sum of squares error	1.10%	0.03%	0.01%	0.004%
Maximum absolute error	2.73%	0.58%	0.36%	0.23%
Number of points	47	47	47	47
Associated figure	3	3	4	5

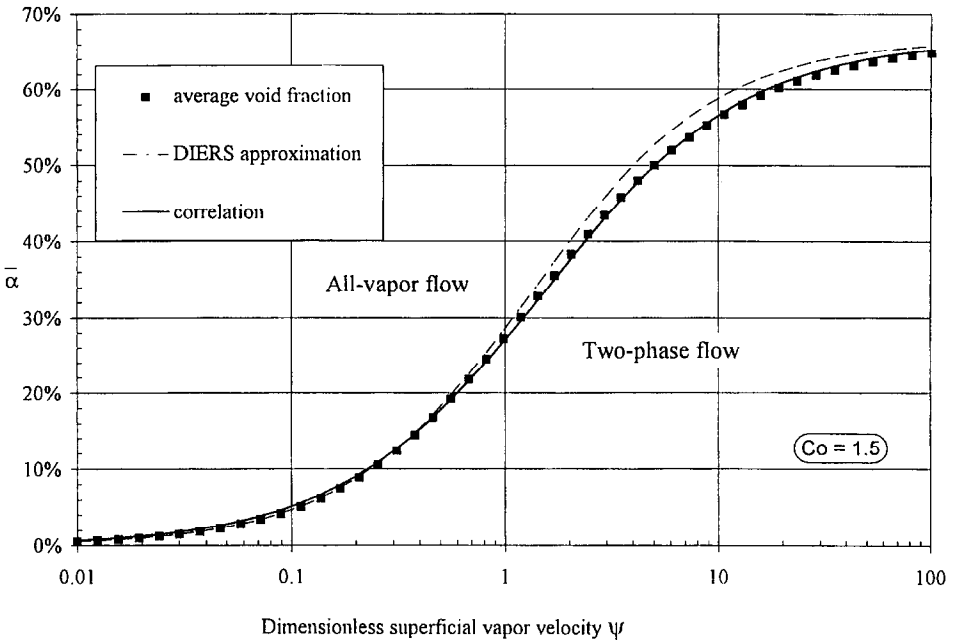

Fig. 3. Churn-turbulent disengagement model results and correlation for vertical cylinder with $Co = 1.5$.

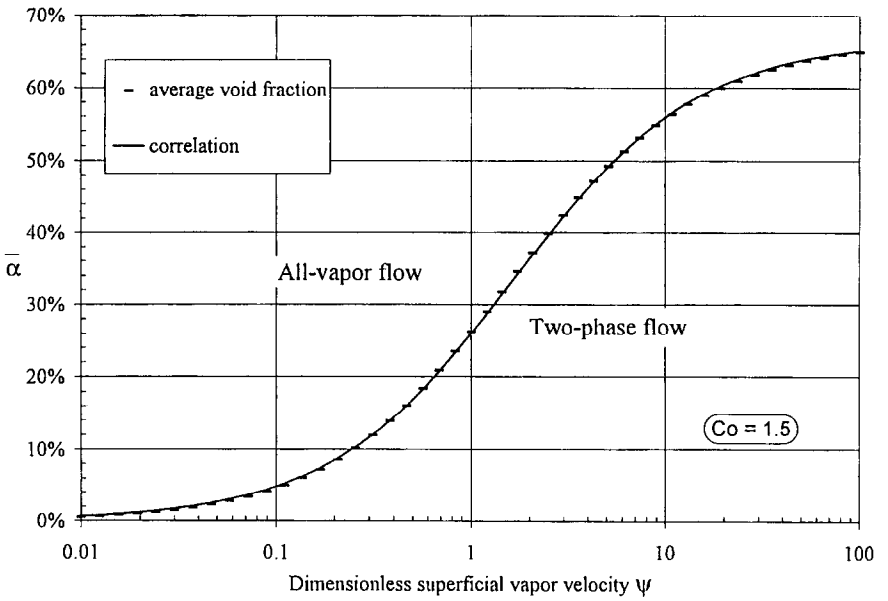

Fig. 4. Churn-turbulent disengagement model results and correlation for a horizontal cylinder with $Co = 1.5$.

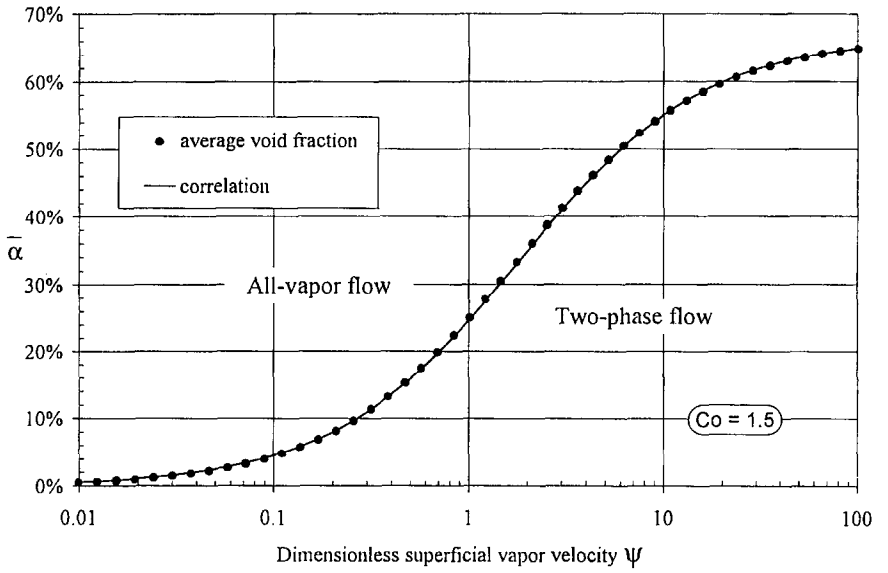

Fig. 5. Churn-turbulent disengagement model results and correlation for a sphere with $Co = 1.5$.

approximation is high. It is noteworthy that the calculated exponent values are the same within the first 2 digits for all three shapes. The correlation is very good, especially in light of the uncertainties associated with the disengagement model.

2.1.2 Correlation values for other Co values

Co values of unity and 1.5 are probably the most commonly used values. However, for completeness, the constant values have been calculated and correlated for intermediate values of *Co*. The correlation equations, selected based on the shape observed, are as follows:

$$K = a + b(Co - 1), \tag{5}$$

$$n = n]_{Co=1} - \frac{1}{c}\left[1 - \exp\left\{\frac{(1 - Co)}{d}\right\}\right]. \tag{6}$$

The latter equation (having the form of an exponential decay) is superior to an alternative power law equation having the form

$$n = n]_{Co=1} - \frac{1}{c}(Co - 1)^d. \tag{7}$$

Table 3 contains the values for the constants a, b, c, and d and the associated correlation errors. Figs. 6, 7, and 8 show the correlation constants of the model results for a vertical cylinder, horizontal cylinder, and sphere, respectively. Fig. 9 shows the correlation results for a sphere for *Co* values of 1.0–2.0. Also shown are the extrapolation of the correlation and an alternative power law correlation. The constant K is no

Table 3
Correlation constants dependent only on *Co* as described in Eqs. (1), (5) and (6)

	a	*b*	$\sqrt{SSE}$* %	$n\|_{Co=1}$	*c*	*d*	$\sqrt{SSE}$ %	Figure
Vertical cylinder	2.00	0.401	0.75	1.00	10.7	5.03	0.70	6
Horizontal cylinder	2.15	0.430	0.75	0.991	12.1	5.66	0.58	7
Sphere	2.34	0.450	0.62	0.982	13.5	6.38	0.33	8 and 9
Power law fit for sphere for Eq. (7)				0.982	9.4	0.467	0.85	8 and 9

* SSE is the sum of squares of the error.

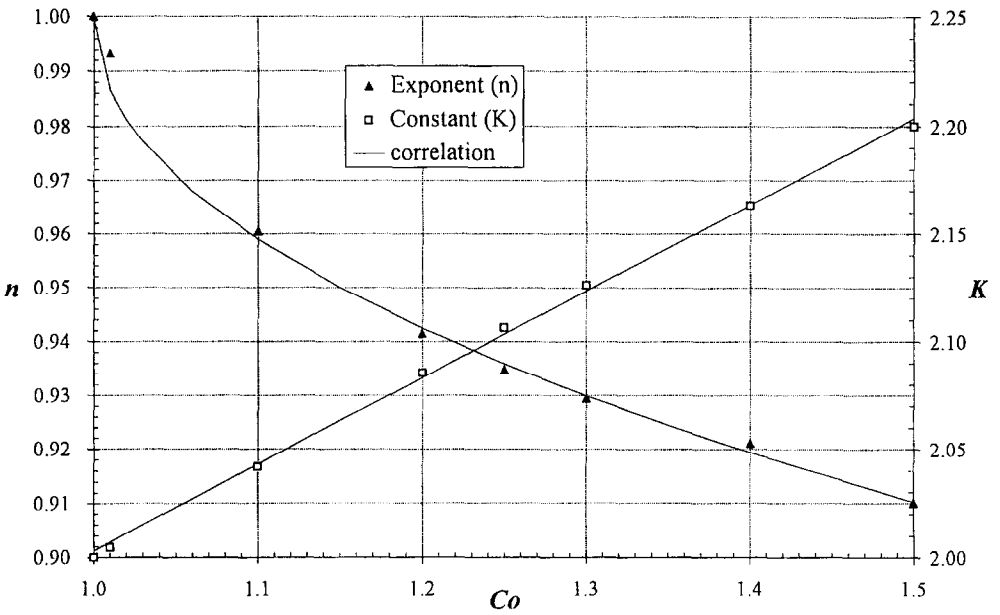

Fig. 6. Vertical cylinder model correlation results for *Co* values between 1.0 and 1.5.

longer a linear function of distribution parameter *Co*. Also, the exponent *n* is not represented well by either relationship at high distribution parameters (*Co* values). This same trend was observed for vertical cylinders and horizontal cylinders. Thus, the correlations should not be extrapolated outside the *Co* range between 1.0 and 1.5.

2.2. Rating calculations

In the rating calculation, the vent size and associated maximum all-vapor venting flow rate are specified, i.e. the engineer has calculated the maximum vapor production rate. Based on this rate, the engineer selects a pressure relief device with an area such

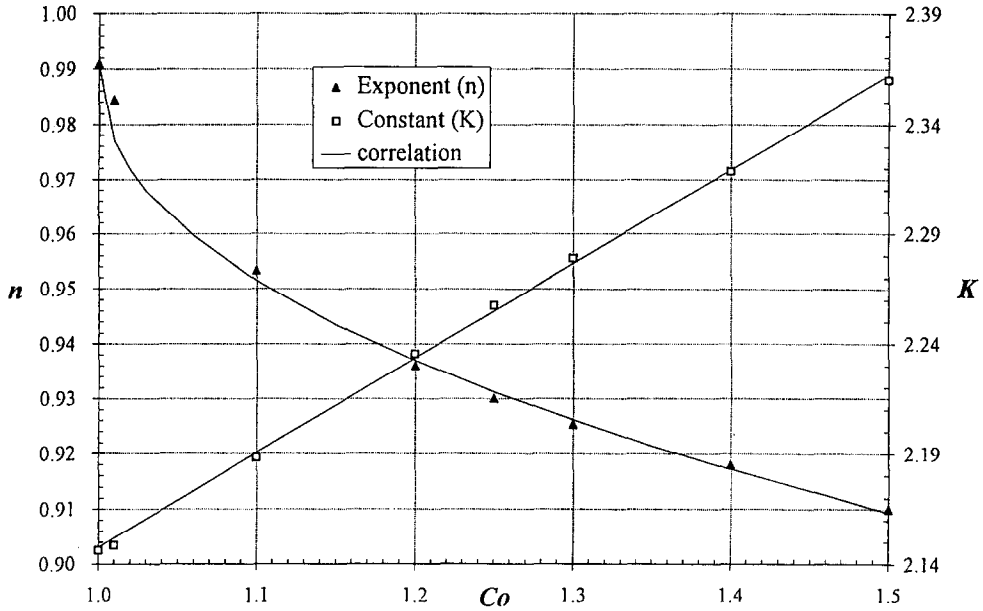

Fig. 7. Horizontal cylinder model correlation results for *Co* values between 1.0 and 1.5.

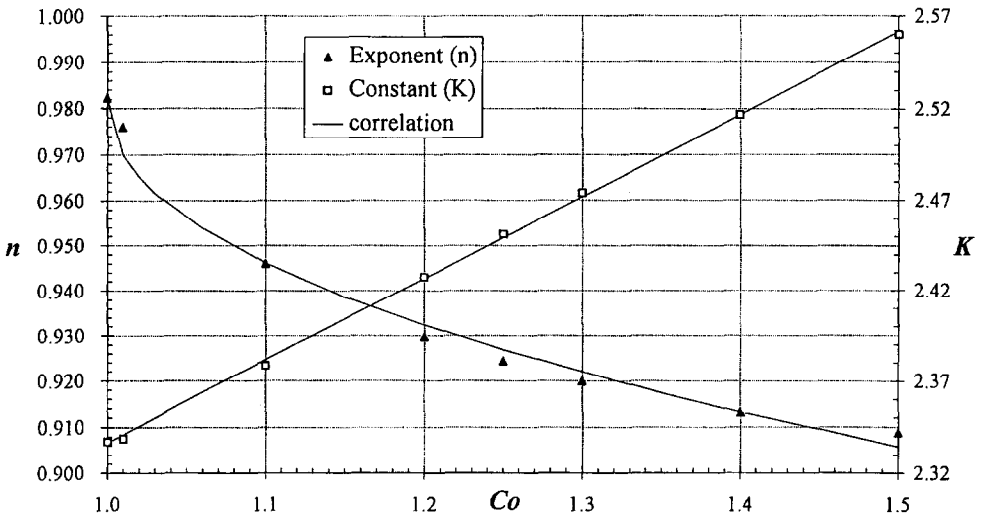

Fig. 8. Sphere model correlation results for *Co* values between 1.0 and 1.5.

that the maximum vent flow exceeds the maximum vapor production rate. Then, the engineer will test at what filling level two-phase flow will occur. The definition for the dimensionless superficial vapor velocity for a constant cross-sectional area vessel [4]

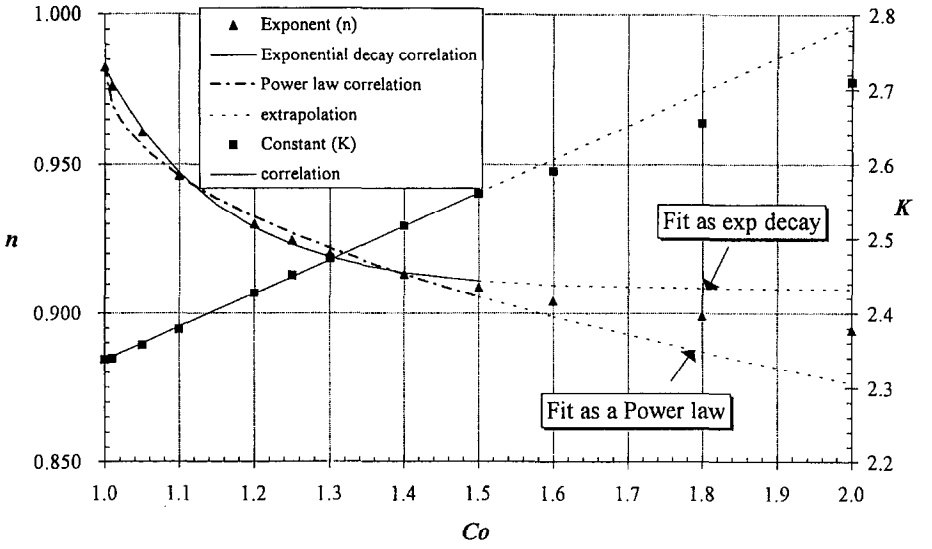

Fig. 9. Sphere model correlation results for Co values between 1.0 and 2.0, correlations fit for model results from Co of 1.0 to 1.5 (including $Co = 1.05$) and extrapolated to 2.0.

is as follows:

$$\psi \equiv \frac{j_{g\infty}}{U_\infty} = \frac{\rho_f}{\rho_g}\frac{q}{\lambda}\frac{H(1-\bar{\alpha})}{U_\infty}. \tag{8}$$

This relationship was used to develop $\bar{\alpha}$ versus ψ curves for horizontal cylinders and spheres. The q/λ accounts for the mass vapor production rate per mass of liquid, which can be replaced by the maximum mass vapor flow rate F divided by the mass of liquid in the vessel $[(1-\bar{\alpha})V_{vessel}\rho_f)]$. Then one obtains

$$\psi \equiv \frac{j_{g\infty}}{U_\infty} = \frac{\rho_f}{\rho_g}\frac{F}{(1-\bar{\alpha})V_{vessel}\rho_f}\frac{H(1-\bar{\alpha})}{U_\infty}. \tag{9}$$

Canceling and rearranging terms results in the following equation:

$$\psi \equiv \frac{j_{g\infty}}{U_\infty} = \frac{F}{\rho_g}\frac{H}{V_{vessel}}\frac{1}{U_\infty}. \tag{10}$$

Finally, with the definitions for volumetric flow rate and average cross-sectional area, one obtains

$$\psi \equiv \frac{j_{g\infty}}{U_\infty} = \frac{F_v/A_{ave}}{U_\infty}, \tag{11}$$

where $F_v(= F/\rho_g)$ is the volumetric vapor flow rate, and $A_{ave}(= V_{vessel}/H)$ is the average cross-sectional area.

This disengagement model is based on the relationship between vapor flux and void fraction. As discussed in Part I [2], the integration can be done either analytically (for constant cross-sectional area vessels) or numerically (for non-constant cross-sectional area vessels). This integration results in an average void fraction versus dimensionless superficial vapor velocity curve which includes the geometry effect (i.e., the influence of the changing cross-sectional area). As seen in Eq. (11), the dimensionless superficial vapor velocity value is based on the vapor exiting the vent.

Note that this conclusion is a correction to Sheppard [1] where an effective cross-sectional area (i.e., $A_{\text{effective}} = V_{\text{liq}}/H_{\text{liq}}$) was suggested rather than this average cross-sectional area. The average cross-sectional area is consistent with the model which assumes that gas production occurs uniformly throughout the liquid phase. Again, the dimensionless superficial vapor velocity, for the all-vapor venting case, is just the maximum vapor flow rate divided by an average cross-sectional area.

In summary, the maximum volumetric vapor production rate must be predicted (e.g., the rate corresponding to the maximum anticipated fill level). Then based on the vessel geometry one can calculate an average cross-sectional area. Using these numbers plus the bubble rise velocity one can calculate the dimensionless superficial vapor velocity ψ value. Then the ψ versus $\bar{\alpha}$ correlation can be used to find the maximum average void fraction. If the vessel average void fraction is larger than this value, all-vapor venting is expected. Then, one can install a vent large enough to handle this vapor flow rate. These calculations are illustrated in the appendix a. If the void fraction is smaller than the maximum average void fraction, two-phase flow will occur for a period during venting. The calculation of the vent line void fraction is discussed in Ref. [6].

3. Conclusions

A simple two-constant correlation is fit for numeric integration data predicting disengagement. The results are based on the pseudo-steady-state assumption and the churn-turbulent drift-flux correlation (implying a continuous liquid phase). This correlation is fit for vertical cylinders, horizontal cylinders, and spheres. The churn-turbulent correlations are within 0.6% of the integration results.

For gassy systems (i.e., vent rating problems) an upper bound on the vapor production rate is required. From this rate, one can calculate the ψ using an average cross-sectional area and bubble rise velocity. Then, the minimum void fraction (i.e., maximum liquid inventory) such that disengagement is predicted can be calculated. Again, the minimum void fraction is the void fraction (or inventory) such that the interface between the two-phase mixture and vapor just swells to the top of the vessel. Liquid entrainment (two-phase flow with the gas phase continuous) is not considered.

Typically for low-viscosity systems, the DIERS recommended churn-turbulent drift-flux correlation and distribution parameter value of 1.5 will be used in pressure relief system design. Both for this distribution parameter value and reasonable alternative distribution parameter values, a simple correlation is presented that will account for both the distribution parameter value and the vessel shape (i.e., vertical

cylinder, horizontal cylinder, or sphere). This correlation will improve the accuracy of disengagement predictions, particularly for horizontal cylinders, and spheres.

Nomenclature

a, b	correlation constants for the coefficient K
A_{ave}	average cross-sectional area of horizontal cylinders and spheres, $(= V_{vessel}/H)$ ft^2 or m^2
$A_{effective}$	effective cross-sectional area of horizontal cylinders and spheres, ft^2. An old definition used in the less correct rating calculation of Sheppard [1] $(= V_{liq}/H_{liq})$
c, d	correlation constants for the exponent n
F	mass relief vent flow capacity, lb/h or kg/h
F_v	volumetric relief vent vapor flow capacity, ft^3/s or m^3/s
g	gravitational constant, ft/s^2 or m/s^2
H	height of the tank, ft or m
K	constant for correlation of $\bar{\alpha}$ and ψ
n	exponent for correlation of $\bar{\alpha}$ and ψ
q	heat generation rate per mass of liquid, Btu/s lb or J/s kg)
U_∞	bubble rise velocity, $(=1.53\sqrt[4]{(\sigma g(\rho_f - \rho_g))/\rho_f^2}$ (for churn-turbulent, Ref. [7]) and $(=1.18\sqrt[4]{(\sigma g(\rho_f - \rho_g)/\rho_f^2})$ (for bubbly, Ref. [7]), ft/s or m/s
V_{vessel}	volume of the vessel, ft^3 or m^3

Greek letters

$\bar{\alpha}$	average void fraction
λ	latent heat of vaporization, Btu/lb or J/kg
Ξ	modified dimensionless superficial vapor velocity, Ref. [8] $= \dfrac{\rho_f}{\rho_g}\dfrac{q}{\lambda}\dfrac{H}{U_\infty} = \dfrac{\psi}{(1-\bar{\alpha})}$
ρ_f	liquid density, lb/ft^3 or kg/m^3
ρ_g	vapor density, lb/ft^3 or kg/m^3
σ	surface tension, dyn/cm or N/m
ψ	dimensionless superficial vapor velocity $= \dfrac{\rho_f}{\rho_g}\dfrac{q}{\lambda}\dfrac{(H(1-\alpha))}{U_\infty}$

Acknowledgements

This research was conducted while the author was a Visiting Scientist at the Safety Technology Institute at the Joint Research Centre in Ispra, Italy. This support by the European Commission (Directorate - General XII - Science Research and Development) is gratefully acknowledged. Input from S.D. Morris, H. Fisher, and the reviewers was very helpful.

Appendix A: Revisiting the rating calculation procedure using the DIERS correlation (after Sheppard [1])

This rating example was originally patterned after Fisher's example [3]. It illustrates the usefulness of this research as a screening tool. The results allow short-cut calculations that indicate the potential for two-phase vent flow. Typically during two-phase pressure relief, process variables (e.g., pressure and temperature) and physical properties (e.g., density and surface tension) are changing quickly and drastically. Therefore, approximate solution is not a replacement for the dynamic simulation needed for most two-phase pressure relief device designs.

A tempered reaction system is assumed. This assumption is necessary in order for the pseudo-steady-state assumption to be reasonable under venting conditions. Also, it is assumed that the churn-turbulent drift-flux correlation describes the system behavior. This assumption is the basis of the entire article. That is, the viscosity is less than 100 cP, and there is no tendency to foam [3]. Since a *Co* of 1.5 was used (best estimate), the maximum average void fraction is 2/3. Fig. 10 is a schematic of the system.

Given conditions

Relief device vapor flow capacity:	43 200 lb/h
Surface tension:	$\sigma = 20$ dyn/cm^2
Other physical properties:	same as water
Burst pressure	100 psig
Rupture disk size:	exactly right
Spherical tank diameter	20 ft
Initial or average void fraction:	20%

1. Relief device vapor flow capacity:

$$F = 43\,200 \text{ lb/hr} = 12 \text{ lb/s}, \qquad F_v = (12 \text{ lb/s})/(0.24 \text{ lb/ft}^3) = 50 \text{ ft}^3/\text{s}.$$

2. Calculate superficial vapor velocity:

$$j_{g\infty} = \frac{F_v}{A_{ave}} = \frac{50 \text{ ft}^3/\text{s}}{4189 \text{ ft}^3/20 \text{ ft}} = 0.24 \text{ ft/s}.$$

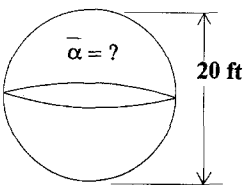

Fig. 10. Schematic of rating problem configuration.

3. Calculate bubble rise velocity:

$U_\infty = 0.61$ ft/s.

4. Calculate dimensionless superficial vapor velocity:

$$\psi_{\text{flow}} \equiv \frac{j_{g\infty}}{U_\infty} = 0.39.$$

5. Calculate the dimensionless superficial vapor velocity for two-phase vent flow onset: From Fig. 5, for an $\bar{\alpha}$ of 0.2, $\psi = 0.7$. This value can be calculated via the correlation given earlier in the paper, by iteration, or algebraic rearrangement. Via algebraic rearrangement, one obtains

$$\bar{\alpha} = \frac{\psi^n}{A + Co\psi^n} = \left[\frac{A}{\psi^n} + Co\right]^{-1} \psi = \left[\frac{A}{1/\bar{\alpha} - Co}\right]^{1/n} = \left[\frac{2.56}{1/0.2 - 1.5}\right]^{1/0.91}, \quad \text{(A.1)}$$

$$\psi_{\text{correlation}} = 0.71. \quad \text{(A.2)}$$

6. Decision criteria: Since $\psi_{\text{correlation}} > \psi_{\text{flow}}$ (i.e., $0.71 > 0.39$), all-vapor venting is predicted. Since all-vapor venting is predicted with an initial void fraction of 20% (i.e., 80% liquid full), more inventory can be held without two-phase vent flow being predicted by this model.

7. Calculate void fraction at disengagement (i.e., maximum liquid inventory). By Fig. 5 at $\psi_{\text{correlation}} = 0.39$, $\bar{\alpha} = 8\%$ (i.e., the maximum liquid inventory is 92%). This value can be calculated via the correlation given earlier in the paper:

$$\bar{\alpha} = \frac{\psi^n}{A + Co\psi^n} = \frac{0.39^{0.91}}{2.56 + 1.5 \cdot 0.39^{0.91}} = 8\%.$$

8. So, if one can guarantee that the vapor production rate is less than the maximum vent flow rate (i.e., 50 ft^3/s in this case) and that the liquid inventory is less than 92% (i.e., an $\bar{\alpha}$ of 8%), then the interface between the two-phase mixture and vapor should be below the vent entrance and thus all-vapor venting should occur.

References

[1] C.M. Sheppard, J. Loss Prevention, 6 (1993) 177.
[2] C.M. Sheppard and S.D. Morris, J. Hazard. Mater., 44 (1995) 111.
[3] H.G. Fisher, Plant/Oper. Progress, 10 (1991) 1.
[4] Fauske and Associates, Inc., Technology Summary, Emergency Relief Systems for Runaway Chemical Reactions and Storage Vessels: A Summary of Multiphase Flow Methods, AIChE/DIERS Publications, New York, 1986.
[5] C.M. Sheppard and S.D. Morris, Two-Phase Flow Disengagement Prediction via Drift-Flux Correlations, Process Engineering Division; Joint Research Center Report, European Commission Ispra, Italy, 1994.
[6] C.M. Sheppard, Drift-flux correlation disengagement models. Part III – Vent stream void fraction prediction for non-constant cross-sectional area vessels also considering entrainment, in preparation.
[7] G.B. Wallis, One Dimensional Two-Phase Flow, McGraw-Hill, New York, 1969.
[8] C.M. Sheppard, Plant/Oper. Prog., 11 (1992) 229.